Journal of Physiology (1997), **502.1**, *pp.*45–60

A quantitative analysis of the activation and inactivation kinetics of *HERG* expressed in *Xenopus* oocytes

Shimin Wang, Shuguang Liu, Michael J. Morales, Harold C. Strauss and Randall L. Rasmusson *

Departments of Medicine, Biomedical Engineering and Pharmacology, Duke University Medical Center, Durham, NC, USA

1. The human *ether à-go-go*-related gene (*HERG*) encodes a K^+ channel that is believed to be the basis of the delayed rectified current, I_{Kr}, in cardiac muscle. We studied *HERG* expressed in *Xenopus* oocytes using a two-electrode and cut-open oocyte clamp technique with $[K^+]_o$ of 2 and 98 mM.

2. The time course of activation of the channel was measured using an envelope of tails protocol and demonstrated that activation of the heterologously expressed HERG current (I_{HERG}) was sigmoidal in onset. At least three closed states were required to reproduce the sigmoid time course.

3. The voltage dependence of the activation process and its saturation at positive voltages suggested the existence of at least one relatively voltage-insensitive step. A three closed state activation model with a single voltage-insensitive intermediate closed state was able to reproduce the time and voltage dependence of activation, deactivation and steady-state activation. Activation was insensitive to changes in $[K^+]_o$.

4. Both inactivation and recovery time constants increased with a change of $[K^+]_o$ from 2 to 98 mM. Steady-state inactivation shifted by ~30 mV in the depolarized direction with a change from 2 to 98 mM K_o^+.

5. Simulations showed that modulation of inactivation is a minimal component of the increase of this current by $[K^+]_o$, and that a large increase in total conductance must also occur.

Cardiac delayed rectified K^+ channels have long been known to be important in repolarization and pacemaker activity (McAllister, Noble & Tsien, 1975; Noble, 1984; Shibata & Giles, 1985; DiFrancesco, 1985; Anumonwo, Freeman, Kwok & Kass, 1992; Campbell, Rasmusson & Strauss, 1992; Wang, Fermini & Nattel, 1993; Muraki, Imiazumi, Watanabe, Habuchi & Giles, 1995; Verhiejck, van Ginneken, Bourier & Bouman, 1995). In cardiac myocytes, at least two types of K^+ channels have been shown to contribute to the development of delayed rectification and repolarization in cardiac muscle. One of these activates slowly (I_{Ks}) and the other activates much more rapidly and shows strong time-dependent rectification (I_{Kr}) (Balser, Bennett & Roden, 1990; Jurkiewicz & Sanguinetti, 1993). In particular, I_{Kr} is believed to have the *HERG* (*ether-à-go-go*-related) gene as its molecular basis because expression of *HERG* results in a channel with distinctive characteristics similar to native I_{Kr} observed in myocytes (Sanguinetti, Jiang, Curran & Keating, 1995, Trudeau, Warmke, Ganetzky & Robertson, 1995*a*). Furthermore, mutations in *HERG* have been linked to a familial form of long QT syndrome (Curran, Splawski, Timothy, Vincent, Green & Keating, 1995) indicating that I_{Kr} is an important contributor to repolarization despite its small size compared with other K^+ currents (e.g. I_{to}, I_{Ks}, and I_{K1}) in many mammalian preparations. Quantitative measurement of this channel has relied on the specificity of block by the Class III antiarrhythmic compounds E-4031 (1-[2-(6-methyl-2-pyridyl) ethyl]-4-(4-methylsulphonyl aminobenzoyl) piperidine), dofetilide and almokalant (Carmeliet, 1992, 1993; Jurkiewicz & Sanguinetti, 1993).

Recently it has been shown that rectification arises from a rapid inactivation process (Smith, Baukrowitz & Yellen, 1996; Wang, Morales, Liu, Strauss & Rasmusson, 1996*b*; Spector, Curran, Zou & Sanguinetti, 1996). Quantitative analysis of activation in the presence of rapid inactivation is critically dependent upon separation of activation from inactivation (Liu, Rasmusson, Campbell, Wang & Strauss, 1996). For example, inactivation of I_{Kr} is faster than channel activation which can alter the apparent time course

* To whom correspondence should be addressed at the Department of Biomedical Engineering, Room 136, School of Engineering, Box 90281, Duke University, Durham, NC 27708-0281, USA.

of current activation (Liu *et al.* 1996). To overcome this problem, Liu *et al.* (1996) examined the development of tail currents, which eliminated inactivation as a factor in this analysis and previously unmeasured properties of I_{Kr} became readily apparent. The most important of these was the observation that activation showed substantial sigmoidal deviation from single-exponential activation and voltage-dependent saturation in its 'on' rate, suggesting the presence of a voltage-independent step in the activation sequence. The sigmoidal delay resulting from multiple states in the activation pathway of I_{Kr} is similar to the activation process of other voltage-gated K^+ channels (Hoshi, Zaggotta & Aldrich, 1994). However, the presence of a major rate-limiting voltage-independent step preceding activation is unique among voltage-gated K^+ channels. These important properties of transient behaviour at positive potentials, sigmoidal activation of tail currents and voltage-insensitive steps in the activation sequence, have not been demonstrated or quantitatively modelled for the HERG channel (Clay, Ogbaghebriel, Paquette, Sasyniuk & Shrier, 1995). In addition, the use of drug-sensitive subtraction and the presence of overlapping K^+ currents limited the voltage range and extracellular $[K^+]$ range for biophysical characterization of the native channel.

Another distinctive property of I_{Kr} and the heterologously expressed HERG current, I_{HERG}, is time-dependent inward rectification. The strong inward rectification of I_{HERG} and I_{Kr} has recently been proposed to result from a time-dependent inactivation-like process (Shibaski, 1987; Sanguinetti *et al.* 1995; Smith *et al.* 1996; Wang *et al.* 1996*b*; Spector *et al.* 1996). This inactivation process has recently been proposed to result from closure of the external mouth of the pore, or C-type inactivation (Smith *et al.* 1996; Schönherr & Heinemann, 1996) and to be insensitive to N-terminal deletion (Spector *et al.* 1996; Schönherr & Heinemann, 1996). However, this inactivation process has not been quantitatively characterized over the physiological range of potentials.

In this study, we measure and quantitatively model the time and voltage dependence of the activation and inactivation processes of HERG. Inactivation of HERG has a strong bell-shaped voltage dependence of inactivation and recovery time constants. Inactivation, but not activation, is altered by $[K^+]_o$. In contrast to inactivation in other K^+ channels, both development and recovery from inactivation are slowed by increased $[K^+]_o$. Our results suggest that inactivation of HERG has a unique intrinsic voltage sensor and a $[K^+]_o$ dependence. These properties differentiate inactivation of HERG from classic C-type inactivation, which is generally voltage insensitive and in which recovery is accelerated by increased $[K^+]_o$ (Hoshi, Zagotta & Aldrich, 1990; Rasmusson, Morales, Castellino, Zhang, Campbell & Strauss, 1995). This suggests that the conformational changes which result in C-type inactivation involve more than superficial external sites which lie outside the membrane field and may involve significant movement of the membrane-spanning domains during C-type inactivation. We also couple this activation model to a quantitative model of HERG inactivation. This complete model reproduces the observed transient behaviour of the expressed current and its activation and inactivation properties. It also demonstrates that the gating properties of I_{HERG} and I_{Kr} are strikingly similar.

METHODS

Mature female *Xenopus laevis* (Xenopus One, Ann Arbor, MI, USA) were anaesthetized by immersion in tricaine solution (1·5 g l^{-1} in 25 mM NaH_2PO_4, pH 6·8). Ovarian lobes were removed through a small incision in the abdominal wall. The follicular layer was removed enzymatically by placing the lobes in a collagenase-containing Ca^{2+}-free OR2 solution (mM: 82·5 NaCl, 2 KCl, 1 $MgCl_2$, 5 Hepes, pH 7·4; 1–2 mg ml^{-1} collagenase, Type I, Sigma). After removal of the ovarian lobe, the frogs were sutured (twice in the abdominal wall and twice in the external skin). The frogs were then allowed to recover in a small water-filled container, with their heads elevated above water level. Once the animal had recovered from anaesthesia, it was placed in a separate aquarium by itself and monitored until healed. Typically, lobes were obtained three times from a single frog. When individual frogs no longer yielded acceptable oocytes, anaesthetized frogs were killed by an overdose of tricaine (20 g l^{-1}). The oocytes were gently shaken for 3 h, with an enzyme solution replacement at 1·5 h, and collagenase activity was then halted as previously described (Comer *et al.* 1994). Defolliculated *X. laevis* oocytes (stage V–VI) were injected with 50 nl cRNA solution prepared as described before (Comer *et al.* 1994), containing up to 50 ng *HERG* cRNA made from plasmids kindly provided by Dr M. Keating at the University of Utah (Curran *et al.* 1995). In some experiments we also used cRNA from plasmids kindly provided by G. Robertson at the University of Wisconsin (Trudeau *et al.* 1995*a*). This clone contained two point mutations in the 5′ end: T595A, yielding V198E, and C607T, yielding P202L (Trudeau, Warmke, Ganetsky & Robertson, 1996*b*), but displayed an identical phenotype compared with the wild-type clone.

Oocytes were voltage clamped using a two-microelectrode 'bath clamp' amplifier (OC-725A, Warner Instruments Corp., Hamden, CT, USA) as has been described in detail elsewhere (Comer *et al.* 1994). Microelectrodes were fabricated from 1·5 mm o.d. borosilicate glass tubing (TW150F-4, WPI) using a two-stage puller (L/M-3P-A, Adams & List Associates, Ltd, Great Neck, NY, USA) filled with 3 M KCl, with resistances of 0·6–1·5 MΩ. During recording, oocytes were continuously perfused with control ND 96 solution (mM: 96 NaCl, 2 KCl, 1 $MgCl_2$, 1·8 $CaCl_2$, 10 Hepes, at pH 7·4, adjusted with NaOH). The 98 mM K^+ solution contained (mM): 98 KCl, 1 $MgCl_2$, 1·8 $CaCl_2$, 10 Hepes, pH at 7·4, adjusted with NaOH. Currents were recorded at room temperature (21–23 °C) and were filtered at 2·5 kHz for the two-electrode voltage clamp recordings. Data were recorded on videotape using an A/D VCR adaptor (model PCM 4/8, Medical Systems Corporation, Greenvale, NY, USA) and digitized using pCLAMP software (Axon Instruments). Unless otherwise stated, raw two-electrode voltage clamp data traces were not leakage or capacitance subtracted.

Where resolution of rapid kinetic components was required, experiments were performed using a cut-open oocyte clamp amplifier

(CA-1a, Dagan Corp., Minneapolis, MN, USA) (Taglialatela, Toro & Stefani, 1992) as described previously (Comer *et al.* 1994). Extracellular solution (ND-96) contained (mM): 96 NaCl, 2 KCl, 1 $MgCl_2$, 1·8 $CaCl_2$, 5 Hepes–NaOH, pH 7·4. High K^+ extracellular solution contained (mM): 98 KCl, 1 $MgCl_2$, 1·8 $CaCl_2$, 5 Hepes–NaOH, pH 7·4, and intracellular solution contained (mM): 98 KCl, 1·8 $MgCl_2$, 1 EGTA, 5 Hepes–NaOH, pH 7·4. Current traces from the cut-open oocyte clamp were leakage and capacitance subtracted using a *P*/4 pulse protocol, unless otherwise noted. Cut-open oocyte clamp data were filtered at 5 kHz. Data are shown as means ± S.E.M. Confidence levels were calculated using Student's paired *t* test.

Data analysis and modelling

Data were digitized and analysed directly using pCLAMP software. Activation time course was analysed from measurement of peak (i.e. after recovery from inactivation) tail currents at negative potentials. The assumption that underlies the analysis of tail currents to characterize activation is that the peak tail current is proportional to the total number of channels which reside in the activated states (i.e. the sum of the open and inactivated states). This is true if *either* of two following assumptions holds true. Assumption A is that the rate of recovery from inactivation is much faster than the rate of deactivation during the P2 pulse. In this case all channels recover from inactivation before appreciable deactivation occurs. The peak current therefore represents the total number of channels activated during the preceding pulse and is an accurate measure of activation time course, regardless of assumptions of independence or coupling between open and inactivated states. Assumption B is that the ratio between open and inactivated channels is relatively constant during the P1 pulse. The peak current during the P2 pulse is a function of the initial conditions and the rate constants at the recovery potential. Subject to the standard assumption that the rate constants are time invariant, the peak current is a function of the total number of activated channels and the ratio between inactivated and open channels. If the ratio between open and inactivated channels is relatively constant then the peak current will simply be a function of the total number of activated channels, regardless of the coupling between open and inactivated states. Since the voltage-dependent recovery and deactivation time constants do not change with P1 pulse durations, the apparent activation time course should be unaffected even if there is some overlap between inactivation and deactivation time constants. Thus, no model-specific assumptions concerning the independence or coupling between open and inactivated state are built into this analysis. For all potentials studied quantitatively in this paper, both Assumptions A and B hold true. At −80 mV, recovery is more than an order of magnitude faster than deactivation, validating Assumption A. At most potentials positive to 0 mV, inactivation is an order of magnitude faster than activation, validating Assumption B. It should be noted that when both assumptions are satisfied, the total possibility for error is reduced dramatically.

Mean activation data were fitted to sequential activation models using custom programs written in Borland C++ implementing a Marquardt optimization procedure similar to that described previously for optimizing a model of I_{To} activation to mean data (Campbell, Rasmusson, Qu & Strauss, 1993). Model simulations were calculated using a fourth order Runge–Kutta algorithm with a variable step size as described previously (Campbell *et al.* 1993) and implemented in Borland C++. Numerical accuracy was confirmed by demonstrating insensitivity to step size.

RESULTS

Activation

HERG expresses an inwardly rectifying K^+-selective current when expressed in *Xenopus* oocytes. The size of the current through the channel is strongly dependent on extracellular K^+ concentration (Trudeau *et al.* 1995; Schönherr & Heinemann, 1996) as shown in Fig. 1*A*, *B* and *C*. For many channels, the concentration of permeant ions alters the gating transitions of the channel and the channel conductance. However, activation of HERG was insensitive to elevation of $[K^+]_o$ from 2 to 98 mM as measured by the lack of a shift in steady-state activation (Fig. 1*D*). The apparent time constant of activation (Fig. 1*E*) measured in the potential range −40 to +20 mV was also insensitive to $[K^+]$ elevation. Steady-state activation was obtained from analysis of peak P2 currents similar to those in Fig. 1*A* and *B*. Peak P2 currents were normalized to those obtained for a P1 potential of +50 mV and plotted as a function of P1 potential to obtain the steady-state activation curve shown in Fig. 1*D*. Steady-state activation was well described by a Boltzmann function with $V_{½}$ values of −21·3 and −23·7 mV and k values of 7·03 and 6·67 mV in 2 and 98 mM K^+_o, respectively, where $V_{½}$ is the membrane potential at half-maximal activation and k is the slope factor. Apparent activation was measured with single exponential fits to the time course of activation in response to the initial P1 depolarization in different concentrations of $[K^+]_o$ (e.g. Fig. 1*A* and *B*) to provide a first approximation to the activation process.

Previous studies of native I_{Kr} have suggested that the activation process of this channel cannot be accurately measured at more depolarized potentials by the method of direct fit to the activation time course (Castellino, Morales, Strauss & Rasmusson, 1995; Liu *et al.* 1996). In addition, the small outward currents carried by this channel make quantitative analysis of the activation process difficult at best at all potentials. To analyse the time and voltage dependence of activation we used an envelope of tails protocol similar to that previously used to analyse activation of native ferret I_{Kr} (Liu *et al.* 1996). Figure 2*A* shows typical current records obtained using this procedure. Briefly, the oocytes were depolarized to the activation potential (P1 = +50 mV, V_h = −80 mV and $[K^+]_o$ = 98 mM) for varying durations of time (Δt). Upon repolarization to −80 mV, a tail current was recorded, the peak amplitude of which was plotted as a function of Δt (Fig. 2*B*). Repeating this protocol for test potentials of 0 to +70 mV in 10 mV steps gave an accurate reconstruction of the time and voltage dependence of activation. The time course of HERG activation was clearly sigmoidal at all potentials and showed slightly more sigmoidal delay than native I_{Kr} from ferret atrium.

The time and voltage dependence of deactivation were measured directly from deactivation tail currents. Oocytes were clamped from a holding potential of −80 mV to a P1

potential of +50 mV for 3 s to activate the current fully. P1 was then followed by a P2 pulse to various potentials (−120 to +50 mV, in 10 mV increments) in the presence of 2 or 98 mM K_o^+ (Fig. 2*C* and *D*). Following repolarization to negative potentials there is a clear delay or 'hook' visible in the tail currents. Such a hook is indicative of rapid recovery from inactivation and/or rectification followed by a slower decay of the current due to deactivation (Shibasaki, 1987; Sanguinetti *et al.* 1995). The mean results are plotted in Fig. 2*E*. Clearly, the deactivation time constants are strongly voltage dependent, suggesting that the open state or the duration of an open burst state (Kiehn, Lacerda, Wible, Sanguinetti, Keating & Brown, 1996) is voltage dependent and is modelled as a voltage-dependent step that communicates directly with the open state, similar to previous findings for I_{Kr} in native myocytes (Liu *et al.* 1996).

To guide our development of a model of the activation process we examined the degree of sigmoidicity of onset by curve fitting of the activation data. We examined the sigmoidicity of the onset of activation using an envelope of tails protocol

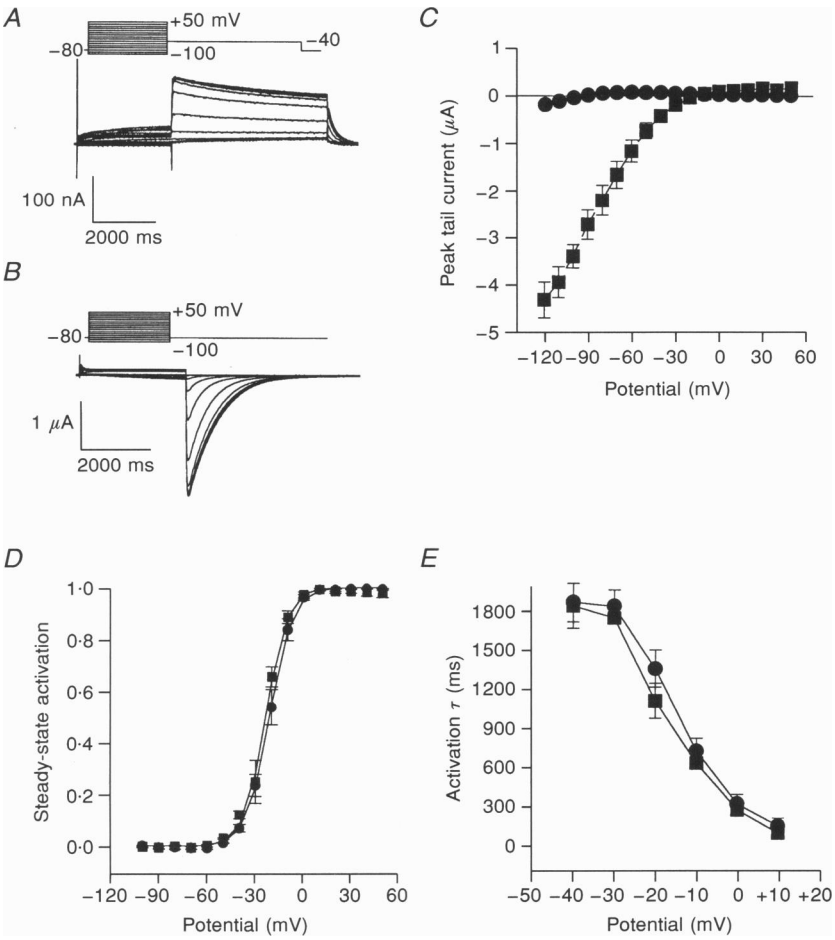

Figure 1. Properties of *HERG* expressed in *Xenopus* oocytes exposed to 2 and 98 mM K_o^+

A, typical I_{HERG} currents recorded in 2 mM K_o^+ in response to a series of depolarizing P1 pulses for 3000 ms to potentials ranging between −100 and +50 mV followed by a 5000 ms P2 pulse to −40 mV (V_h = −80 mV). *B*, currents recorded from the same oocyte as in *A* but with 98 mM K_o^+ in response to a series of depolarizing P1 pulses for 3000 ms to potentials ranging between −100 and +50 mV and returned directly to V_h (−80 mV). *C*, fully activated peak tail current. Currents (not shown) were recorded from a P1 pulse to +50 mV for 3000 ms to fully activate the channel, followed by a P2 pulse to different potentials ranging between −120 and +50 mV to elicit tail currents (V_h = −80 mV) in 2 and 98 mM K_o^+. *D*, mean fully activated peak tail currents. Data obtained by using the protocol shown in *A* and *B* were normalized by the maximal outward current (P1 = +50 mV; paired data, n = 4). The continuous lines represent fits of the Boltzmann distribution to the data. $V_{½}$ was −21·3 and −23·7 mV and k was 7·03 and 6·67 mV for 2 and 98 mM K_o^+, respectively. *E*, voltage and concentration dependence of apparent activation time constants determined using direct fit analysis to P1 currents. Activation time courses similar to those during P1 of *A* and *B* were fitted to a single exponential equation and the mean time constants (paired data, n = 4) were plotted against activation potentials. No significant $[K^+]_o$-dependent change in apparent activation rate was found. In all panels, ● denotes 2 mM K_o^+ and ■ denotes 98 mM K_o^+.

similar to that described above except that the activation pulse was preceded by a prepulse to −120 mV for 400 ms. This prepulse was employed to maximize the degree of sigmoidicity. Sigmoidicity is maximized because the resting potential may not reflect a fully deactivated channel. Additional closed states, and increased sigmoidal delay, may be achieved by hyperpolarization, as demonstrated by Cole & Moore (1960). The activation potential was to +50 mV. We then fitted this activation time course with a series of simple activation models as follows:

$$C_1 \rightarrow O$$
$$C_1 \rightarrow C_2 \rightarrow O$$
$$C_1 \rightarrow C_2 \rightarrow C_3 \rightarrow O$$
$$C_1 \rightarrow C_2 \rightarrow C_3 \rightarrow C_4 \rightarrow O$$

The fit for each of these models is shown in Fig. 3; those of mean data are shown in the left-hand column of the figure and the residual errors are plotted in the right-hand column. The model with only one closed state obviously fits the data poorly and the residual error plot shows the characteristic behaviour of a model fit which is of too low an order. The error resulting from the fit to the data showed systematic behaviour, first being negative, then becoming positive and finally returning to negative values. These runs in the sign of the error can be used as a measure of the goodness of fit for a particular set of data. We used a test based on runs above and below the data fit. If the probability that the distribution of runs above and below the data was due to a random distribution and was less than 0·05 then the model was rejected in favour of a higher order formulation.

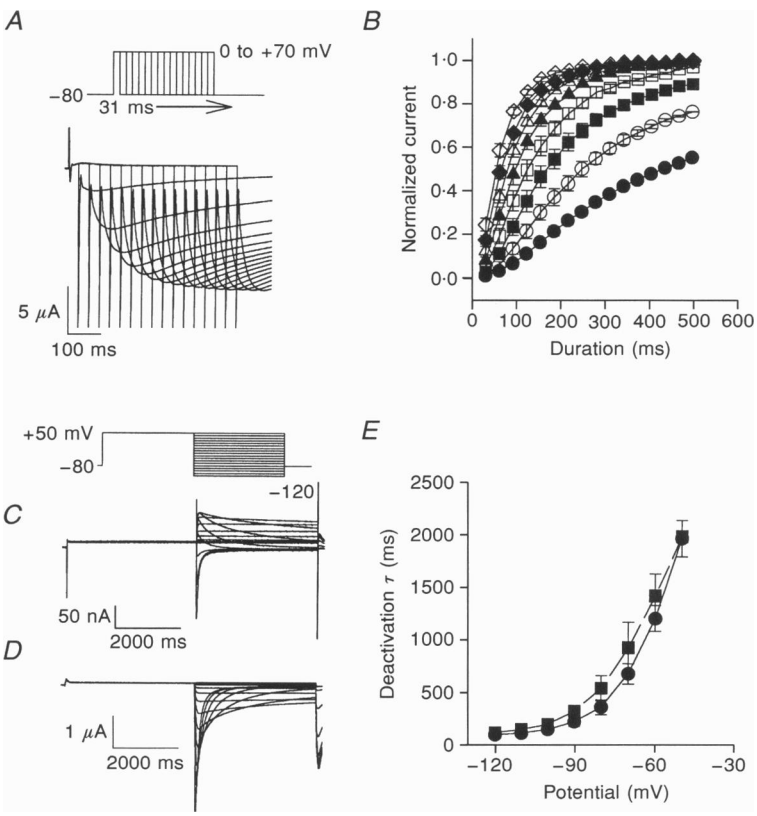

Figure 2. Kinetic properties of activation and deactivation of I_{HERG}

A, activation time course estimated using tail current measurements. Representative tail currents were elicited by depolarizations to +60 mV from a holding potential of −80 mV using different P1 durations. For a complete set of measurements, oocytes were held at −80 mV and then stepped to a P1 potential (0 to +70 mV) for varying periods of time before repolarization to −80 mV. Experiments were performed in 98 mM K_o^+. *B*, mean activation time course of peak tail currents obtained for pulses to varying P1 potentials. Currents were measured as peak currents during repolarization to −80 mV and normalized to the maximum inward tail current measured following various periods of depolarization to +70 mV (data plotted as means ± S.E.M., $n = 3$; ●, ○, ■, □, ▲, △, ◆ and ◇ denote 0, 10, 20, 30, 40, 50, 60 and 70 mV, respectively). *C*, current traces used to measure deactivation time course in 2 mM K_o^+. The holding potential was −80 mV. A depolarizing prepulse to +50 mV of 3000 ms duration delivered to the oocyte was applied before subsequently stepping to various potentials (+50 to −120 mV in 10 mV increments). *D*, data from the same oocyte as *C* and using the same protocol but with 98 mM K_o^+. *E*, mean voltage dependence of deactivation time constants from experiments *C* and *D*. The mean time constants from four experiments were plotted against deactivation potentials. ● denotes 2 mM K_o^+ and ■ denotes 98 mM K_o^+.

Although the fit of the two closed state model provided a more appealing visual fit to the data, examination of the systematic error showed that it too was not adequate to describe the data. The fit to the data for a three state model could not be rejected, and higher order models failed to show substantial improvement in the visual quality of the fit, the systematic distribution of error or the total residual error. Therefore, for further analysis and model construction we chose a three closed state model for activation.

Another finding concerning activation of I_{Kr} in native myocytes was that the voltage dependence of activation suggested a voltage-insensitive step that became rate limiting at positive potentials. The evidence for such a step was that the rate of activation at very positive potentials did not increase with increasing depolarization (Liu *et al.* 1996). As can be seen in Fig. 2*B*, the time to half-activation is approaching a constant value although it does not quite become constant at the potentials studied. Since the data in Fig. 2*B* suggest that the decrease in half-activation time was due to a reduced degree of sigmoidal delay, we examined the late phase of activation (Hoshi *et al.* 1994). The data in Fig. 4*A* are the activation time courses from Fig. 2*A* beginning at time $t = 93$ ms. The continuous lines are single exponential fits to the data during the late phase of depolarization. The late time constants of activation are plotted in Fig. 4*B*. As can be seen from this plot, the late phase of activation becomes voltage insensitive at positive potentials, reaching an asymptotic value of 68 ± 10 ms as estimated from the fitted exponential in Fig. 4*B*. This type of voltage dependence of the late component suggests that activation includes a voltage-insensitive step (Hoshi *et al.* 1994).

Following the example of the kinetic characterization of the I_{Kr} current in ferret atrial myocytes, we modelled the activation process of I_{HERG}. The basic model we used was an extension of the one proposed for I_{Kr} in native ferret

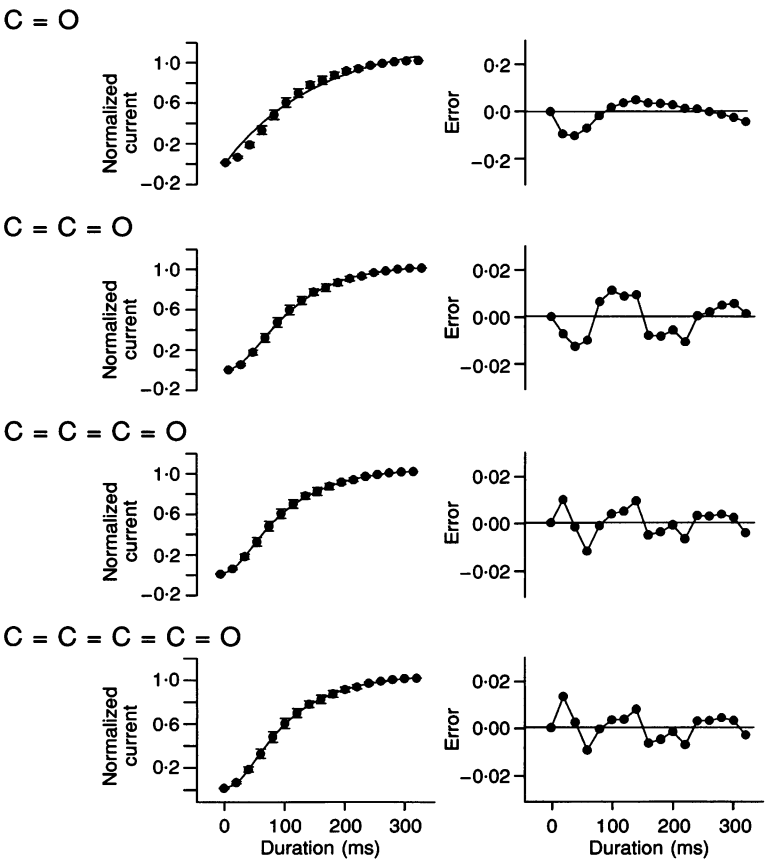

Figure 3. Analysis of the degree of sigmoidicity of activation

Oocyte currents were measured with a tail current procedure similar to that shown in Fig. 2*A*. The only difference was that a prepulse to −120 mV for 400 ms was applied prior to activation of the current to maximize any apparent Cole–Moore shifts (Cole & Moore, 1960) in activation sigmoidicity. The left-hand column shows the mean activation time course data for an activation potential of +50 mV with the order of the model and resulting fit. The right-hand column shows the distribution of the data error about the fitted curve. The systematic distribution of this error was used as a criterion for rejection of models. The distribution of errors for the one and two closed state models was statistically significantly different from that expected from a purely random distribution with a $P < 0{\cdot}05$ using a test based on runs above and below the mean.

Table 1. Summary of HERG channel dynamic characteristics

Activation	
$\alpha_{a0} = 0{\cdot}022348\exp(0{\cdot}01176\,V_m)$ ms^{-1}	
$k_f = 0{\cdot}023761$ ms^{-1}	
$\alpha_{a1} = 0{\cdot}013733\exp(0{\cdot}038198\,V_m)$ ms^{-1}	
$\beta_{a0} = 0{\cdot}047002\exp(-0{\cdot}0631\,V_m)$ ms^{-1}	
$k_b = 0{\cdot}036778$ ms^{-1}	
$\beta_{a1} = 0{\cdot}0000689\exp(-0{\cdot}04178\,V_m)$ ms^{-1}	
Inactivation	
2 mM KCl	98 mM KCl
$\alpha_i = 0{\cdot}090821\exp(0{\cdot}023391\,V_m)$ ms^{-1}	$\alpha_i = 0{\cdot}030819\exp(0{\cdot}02459\,V_m)$ ms^{-1}
$\beta_i = 0{\cdot}006497\exp(-0{\cdot}03268\,V_m)$ ms^{-1}	$\beta_i = 0{\cdot}012687\exp(-0{\cdot}01402\,V_m)$ ms^{-1}

V_m is the membrane potential in millivolts. The other terms are explained in the text.

myocytes (Liu *et al.* 1996). As suggested by the voltage dependence of deactivation tails, the final closed to open transition was modelled as a voltage-dependent step. To account for the saturation in rate of the late phase of activation, this step was preceded by a voltage-insensitive step, similar to that for I_{Kr}. In addition, the lack of saturation in the sigmoid delay in activation kinetics suggests that an additional weakly voltage-dependent step might precede the voltage-insensitive activation step. Therefore, the activation model used was of the form:

$$C_0 \underset{\beta_{a0}}{\overset{\alpha_{a0}}{\rightleftharpoons}} C_1 \underset{k_b}{\overset{k_f}{\rightleftharpoons}} C_2 \underset{\beta_{a1}}{\overset{\alpha_{a1}}{\rightleftharpoons}} O$$

where C_0, C_1 and C_2 are the closed states in the activation pathway, O is the open and conducting state, α_{a0} and α_{a1} are the forward voltage-dependent rate constants, β_{a0} and β_{a1} are the backward voltage-dependent rate constants, k_f is the voltage-insensitive forward rate constant and k_b is the voltage-insensitive backward rate constant (numerical values are given in Table 1). This model fitted well to the mean activation time course data, the steady-state activation data and the deactivation data in the negative range of potentials. As shown in Fig. 5, the model matched the experimentally observed data closely. The saturating forward time constant $1/k_f$ was 42 ms (see Table 1) which was much slower than the final step ($1/\alpha_{a1}$, ~5 ms), slower than the initial weakly voltage-dependent step ($1/\alpha_{a0}$, ~20 ms) and was in

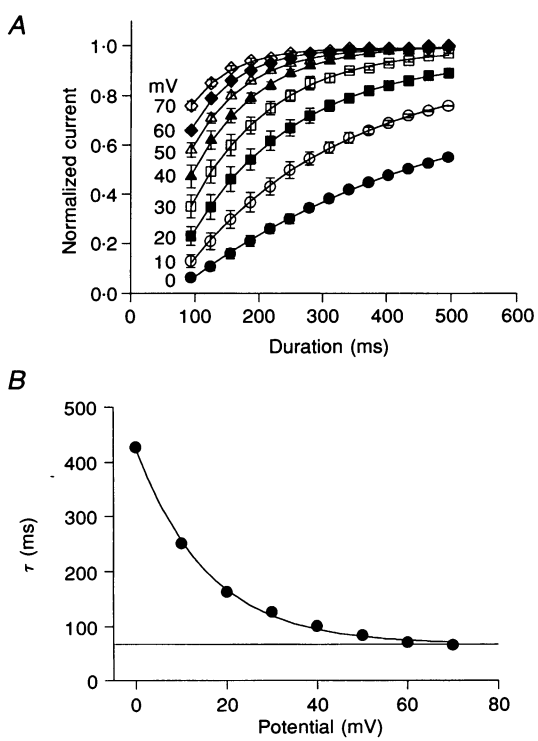

Figure 4. Apparent saturation in the late phase of activation at positive potentials

A, the data from Fig. 2*B* were truncated to begin at $t = 93$ ms to emphasize the late phase of activation. This late phase was fitted with a single exponential. *B*, the time constants from *A* are plotted as a function of test potential. The time constants of activation showed an exponential dependence on membrane potential as shown by the fitted curve. However, this exponential did not decay to zero at positive potentials. Instead it reached an asymptotic value of 68 ± 10 ms (shown as a straight line). This suggests the existence of a relatively voltage-insensitive step which becomes dominant at very positive potentials.

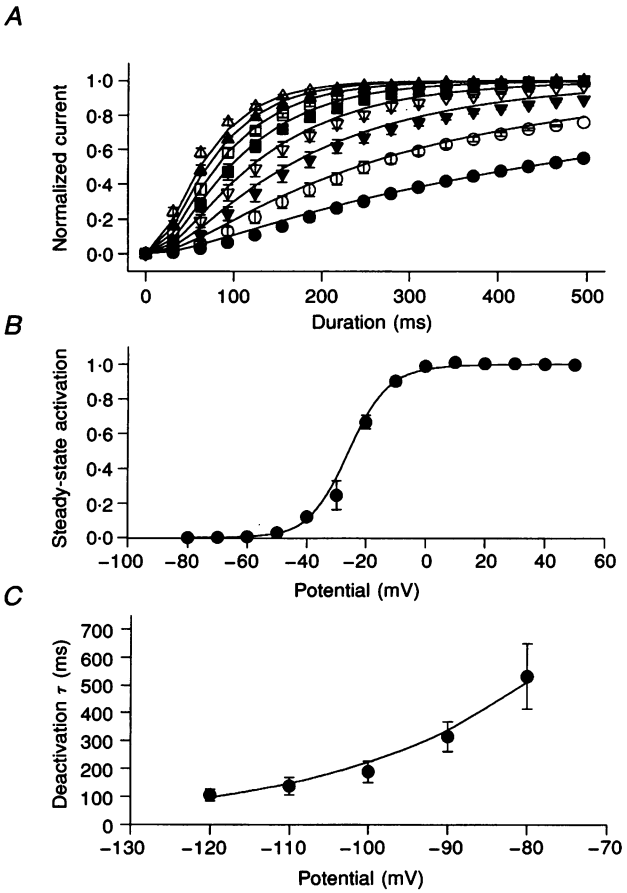

Figure 5. Simultaneous fitting of the three closed state activation model to the mean activation data

A, fit (continuous curves) to activation time course: ●, 0 mV; ○, 10 mV; ▼, 20 mV; ▽, 30 mV; ■, 40 mV; □, 50 mV; ▲, 60 mV; △, 70 mV. *B*, the fit to steady-state activation in 98 mM KCl. *C*, the fit to deactivation time constants in 98 mM KCl. Data from all three panels were used simultaneously during optimization to constrain model parameters. Symbols represent mean experimental data. Continuous lines are fitted results. For activation time course and steady-state activation, the fitting procedure optimized an implementation of the linear four state model. Equations and optimized parameter values are given in Table 1.

reasonable agreement with the single exponential late fit to the data of 68 ± 10 ms measured experimentally.

Inactivation

The rectification properties of I_{HERG} expressed in *Xenopus* oocytes is largely due to rapid inactivation. Despite the rapid kinetics of this inactivation mechanism, it has been demonstrated that it is not an N-type mechanism but is presumed to be due to a closure of the external mouth of the channel, or C-type mechanism (Smith *et al.* 1996). The 'on' rate of this rapid inactivation shows a strong sensitivity to $[K^+]_o$ as predicted for a C-type mechanism. On this basis, it has been proposed that strong dependence of the size of this current on $[K^+]_o$ is due to modulation of inactivation. To

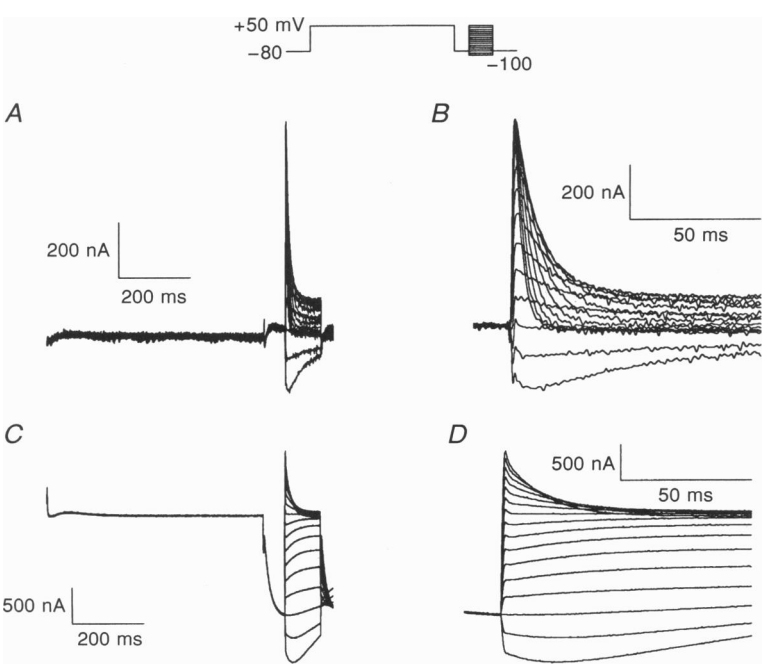

Figure 6. Development of inactivation at positive potentials

A, currents elicited during a three-pulse protocol using the cut-open oocyte clamp technique and 2 mM K_o^+. A 600 ms P1 pulse to +50 mV was applied, followed by a P2 pulse to −80 mV for 60 ms to remove inactivation without allowing deactivation to occur, followed by a P3 pulse to potentials from −100 to +50 mV. *B*, currents during the P3 pulse of *A* expanded to show the time dependence on rate of inactivation. *C*, currents elicited from the same oocyte as *A*, but with 98 mM K_o^+. *D*, currents during the P3 pulse of *C* expanded to show time dependence on rate of inactivation.

evaluate this proposal in a quantitative fashion, we characterized the time and voltage dependence of HERG inactivation. As this inactivation process is very rapid, we used the cut-open oocyte technique (Taglialatela *et al.* 1992) to resolve inactivation kinetics. We measured the time and voltage dependence of inactivation directly, using a three-pulse protocol as described previously. A P1 pulse to +50 mV was initially applied for 600 ms to activate *HERG* fully, which was followed by a P2 pulse to −80 mV for 60 ms to remove inactivation without allowing sufficient time for significant deactivation to occur ($\tau > 500$ ms at −80 mV). A final P3 pulse was then applied to different potentials from −100 to +50 mV. An example of currents recorded using this protocol for a P3 pulse to +50 mV is shown in Fig. 6*A*. Representative currents (for potentials of −100 to +50 mV) during P3 are shown on an expanded scale in Fig. 6*B*. Repeating the pulse protocol in the presence of 98 mM K_o^+ in the extracellular chamber greatly increased the current and slowed the inactivation rate (Fig. 6*C* and *D*). The time constants of development of inactivation during P3 from the same voltage clamp protocol were measured directly by fitting single exponential curves to current decay in the range −60 to +50 mV.

Recovery from inactivation was also measured using protocols similar to those described for I_{Kr} and I_{HERG} (Sanguinetti & Jurkiewicz, 1990; Sanguinetti *et al.* 1995; Liu *et al.* 1996) and using the cut-open oocyte clamp technique. Oocytes were stepped from a holding potential of −80 mV to a P1 potential of +50 mV for 600 ms to activate and then inactivate the current. This was followed by a P2 pulse of different amplitudes (−120 to +40 mV in 10 mV increments) as shown in Fig. 7*A*. Oocytes were then exposed to 98 mM K_o^+ and the procedure was repeated (Fig. 7*B*). Surprisingly, the rate of recovery from inactivation was greatly slowed, contrary to the behaviour also previously described for C-type inactivation in Kv1.4 channels (Rasmusson *et al.* 1995). To quantify the change in the rate of recovery from inactivation, the initial increase in tail current during P2 was fitted to an exponential. In potential ranges where deactivation overlapped with recovery from inactivation, a two-exponential fit was used to separate the two components. The mean time constants for recovery from inactivation are plotted in Fig. 8*B* (filled symbols).

Steady-state inactivation was also measured from the same protocol as in Fig. 6 as described previously for I_{Kr}. Briefly, the steady-state inactivation relationship was calculated as the ratio of the currents measured 100 ms after the beginning of P3 to the instantaneous currents measured at the beginning of P3 in Fig. 6 for potentials positive to −80 mV. This measurement estimated inactivation relative to steady-state inactivation at −80 mV. The value of steady-state inactivation for more negative potentials was obtained by estimating the additional relief of inactivation by hyperpolarizing P3 pulses from −80 to −100 mV as described in the legend of Fig. 6. These data showed a strong shift of steady-state inactivation to more positive potentials with increasing $[K^+]_o$ (Fig. 8*A*).

We examined the relationship between the experimentally determined kinetics of inactivation and the measured steady-state inactivation for both 2 and 98 mM K_o^+ by fitting both sets of data with simple voltage-dependent (Hodgkin & Huxley, 1952) type rate constants. As can be seen from the smooth fits to the mean data (Fig. 8) such a simple first order model fits the data obtained at both 2 and 98 mM K_o^+ well. This fitting procedure shows that despite an apparently equal slowing of forward and backward rate constants the kinetic data are consistent with an ~30 mV shift with increased $[K^+]_o$.

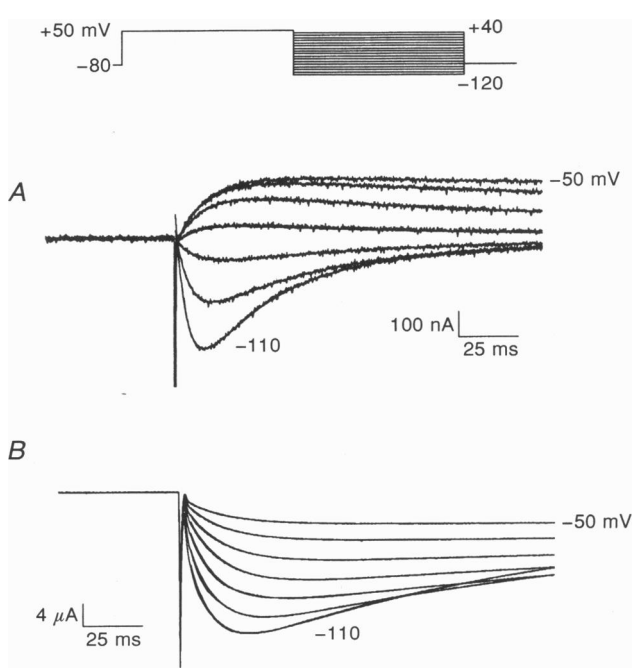

Figure 7. Measurement of recovery from inactivation of I_{HERG}

A, oocytes were clamped using the cut-open oocyte clamp technique. A preconditioning pulse to +50 mV was applied for 600 ms to allow the current to fully activate and inactivate (this portion of the record is truncated in order to make the recovery process more visible). Recovery was observed as the time-dependent initial increase in current at potentials varying between −50 to −110 mV. Continuous lines are the double exponential fits to the current from the end of the capacitive transient to the end of the tail currents, giving time constants of recovery from inactivation. The slower time constant was of opposite amplitude and was assumed to be due to deactivation. *B*, current traces from the same cell with the same voltage clamp protocol as in *A* but with $[K^+]_o$ of 98 mM.

Drawing from the example of the gating characterization of ferret I_{Kr} we combined our activation model with our inactivation model in a linear scheme as follows:

$$C_0 \underset{\beta_{a0}}{\overset{\alpha_{a0}}{\rightleftharpoons}} C_1 \underset{k_b}{\overset{k_f}{\rightleftharpoons}} C_2 \underset{\beta_{a1}}{\overset{\alpha_{a1}}{\rightleftharpoons}} O \underset{\beta_i}{\overset{\alpha_i}{\rightleftharpoons}} I$$

Model 1

The model parameter values and equations are given in Table 1. This model was combined with the previously reported non-linear instantaneous current–voltage relationship (Wang *et al.* 1996*b*) for this channel at each concentration to produce the simulated currents shown in Fig. 9. In these simulations the instantaneous current used was derived from the previously measured instantaneous *I–V* relationship for this channel expressed in *Xenopus* oocytes (Wang *et al.* 1996*b*). Figure 9*A* shows I_{HERG} in response to a series of depolarizing pulses (−100 to 50 mV in 10 mV increments) for 3 s from a holding potential of −80 mV and returned to a deactivation potential of −40 mV for 5 s in 2 mM K_o^+. Figure 9*C* shows the simulated currents predicted by the model for the same protocol. Figure 9*B* shows measured I_{HERG} in response to a series of depolarizing pulses (−100 to +50 mV in 10 mV increments) for 3 s from a holding potential of −80 mV and returned to a deactivation potential of −80 mV for 3 s in 98 mM K_o^+. Figure 9*D* shows the simulated currents for the same protocol. These simulations show that the model closely reproduces the experimentally observed time-dependent rectifying behaviour.

Increased $[K^+]_o$ has been reported to increase the magnitude of both I_{HERG} and I_{Kr}. For I_{HERG} it has been suggested that this increase in total current is due to the effects of $[K^+]_o$

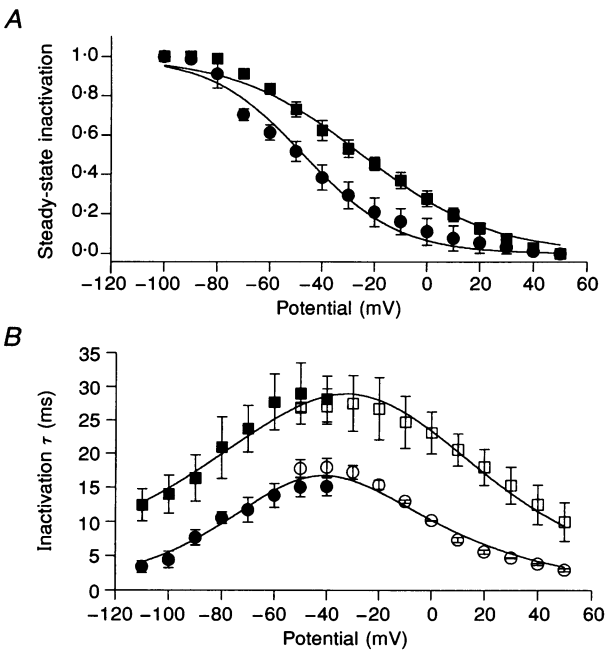

Figure 8. Mean inactivation data and model fit

A, steady-state inactivation relative to the degree of inactivation at −80 mV was calculated as the ratio of currents measured 100 ms after the onset of the P3 pulse (see Fig. 6 and Liu *et al.* 1996) to the instantaneous currents measured at the same potentials in 2 (●) and 98 mM (■) K_o^+. The resulting ratios were then normalized to the degree of inactivation at −80 mV which was measured as the time-dependent increase in current relative to that occurring at −100 mV during the P3 pulse. Saturation in the degree of steady-state inactivation was observed in the range −70 to −100 mV in 98 mM K_o^+ and −70 to −100 mV in 2 mM K_o^+, indicating that relief of inactivation was complete at −100 mV in both cases. No correction was applied for overlapping deactivation because the inactivation and deactivation time constants were separated by over an order of magnitude in this range of potentials and any overlap would be further reduced if inactivation and deactivation were coupled through obligatory-channel opening. Steady-state inactivation was fitted with an $\alpha_i(V_m)$ and $\beta_i(V_m)$ ($Inact_{ss} = 1/\{1 + \alpha_i(V_m)/\beta_i(V_m)\}$) to this data and simultaneously with the data in *B*. Data in 2 and 98 mM K_o^+ were fitted independently and yielded a separate set of parameter estimates (see Table 1). *B*, voltage dependence of inactivation time constants. Open symbols are time constants of development of inactivation (Fig. 6 and Wang *et al.* 1996). Filled symbols are recovery time constants obtained by fitting the current traces described above. ○ and ●, 2 mM KCl; □ and ■, 98 mM KCl. Data shown are means ± S.E.M. (paired data, $n = 4$). The continuous line represents the results of simultaneous fitting of $\alpha_i(V_m)$ and $\beta_i(V_m)$, where $\tau_i = 1/(\alpha_i(V_m) + \beta_i(V_m))$ and $\alpha_i(V_m) = A_3 \exp(A_4 V_m)$ and $\beta_i(V_m) = B_3 \exp(B_4 V_m)$.

on inactivation (Spector *et al.* 1996; Wang, Trudeau & Robertson, 1996*a*; Yang, Snyders & Roden, 1996) while the instantaneous current–voltage relationship is thought to be uninvolved. However, others have reported that increased $[K^+]_o$ alters the instantaneous *I–V* relationship for this channel as well (Wang *et al.* 1996*b*). In addition, Shibasaki (1987) demonstrated that I_{Kr} single channel conductances are strongly sensitive to $[K^+]_o$. We examined the ability of the measured $[K^+]_o$ sensitivity of inactivation to increase current magnitude using model simulations. For these simulations, we used an identical linear conductance for both 2 and 98 mM K_o^+ and altered kinetic parameters of inactivation. The linear approximation should be valid in the negative range of potentials for this channel (Smith *et al.* 1996; Spector *et al.* 1996; Wang *et al.* 1996*b*). Figure 10*A* shows the simulated currents for a channel which is at steady state at −80 mV, then stepped to +50 mV for 3 s to activate the current and then stepped to various potentials (−120 to +40 mV in 10 mV increments) for 3 s to simulate tail currents in 2 mM K_o^+. Figure 10*B* shows the identical simulations, but with inactivation parameters compatible with 98 mM K_o^+. Figure 10*C* shows the peak tail current *I–V* relationship for the two simulations. Mean experimental peak tail current data taken from the same protocol are shown in Fig. 10*D*. All currents were normalized to the value of the peak tail current measured at −80 mV in 2 mM K_o^+. The change observed experimentally was much larger (by a factor of approximately eight) than the changes predicted solely on the basis of altered inactivation. These simulations suggest that changes in the single-channel conductance contribute to the total activation due to increasing extracellular $[K^+]_o$.

Another important feature of the linear model of I_{Kr} was the appearance of a transient component (Liu *et al.* 1996). The simulations in Fig. 11*A* show the predicted currents during the 'on' pulses from a holding potential of −80 mV to potentials between +20 and +50 mV in 2 mM K_o^+. Figure 11*B* shows the experimental records in 98 mM K_o^+ from an oocyte subjected to the same protocol. The model reproduces the main characteristics of the experimentally recorded I_{HERG}, including a very small transient component observed at very positive potentials in 2 mM K_o^+ (Fig. 11*C*). This transient component becomes much larger in both the model and the experimental data when $[K^+]_o$ is 98 mM as shown in Fig. 11*B* and *D*.

DISCUSSION

This paper describes a quantitative analysis of the activation and inactivation properties of the macroscopic current of *HERG* expressed in *Xenopus* oocytes. Partial kinetic descriptions of some properties of this current have appeared before, but this is the first complete general model characterization of both activation and inactivation properties. The similarities in gating characteristics to those

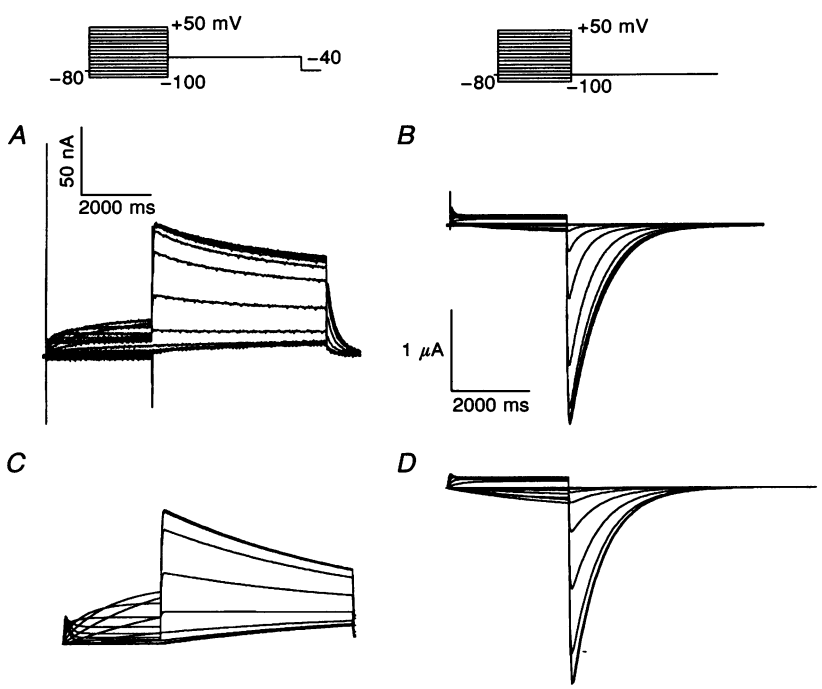

Figure 9. Comparison of data and model for 2 and 98 mM K_o^+

A, typical I_{HERG} recorded in 2 mM K_o^+ in response to a series of depolarizing P1 pulses for 3000 ms to potentials ranging between −100 and +50 mV followed by a 5000 ms P2 pulse to −40 mV (V_h = −80 mV). *B*, currents recorded from the same oocyte as *A* but with 98 mM K_o^+ in response to a series of depolarizing P1 pulses for 3000 ms to potentials ranging between −100 and +50 mV and returned directly to V_h (−80 mV). *C* and *D*, model simulations of the current records described in *A* and *B* above.

previously identified for ferret atrial I_{Kr} help validate the link between *HERG* and I_{Kr}.

Activation

Measurement of the activation process using the envelope of tails procedure allowed quantitative analysis of the activation time course. Activation showed a sigmoidal time dependence. Other evidence suggested a relatively voltage-insensitive step during activation that was similar to that observed for ferret atrial I_{Kr}. The deactivation tail currents suggested that the open state communicates directly with a voltage-sensitive rate-limiting final transition from the closed state. We should note that the open state as described in this paper is an aggregate conducting state. By aggregate conducting state we mean that it may be a single open conformation or it may be an aggregate of conformations, e.g. a bursting state. If the open channel shows bursting behaviour, as has been previously suggested in single channel studies (Kiehn, Lacerda, Wible, Sanguinetti, Keating & Brown, 1996), then a brief-lived closed state may exist as the final step in the activation pathway.

The analysis of the sigmoidal activation of I_{Kr} has indicated that at least two closed states are required to reproduce the kinetic behaviour of the current quantitatively. However, Liu *et al.* (1996) could not rule out the possibility that additional voltage-sensitive and voltage-insensitive steps exist in the activation process (i.e. closed state transitions). In fact, they proposed that small deviations between the model and their data suggested that additional activation steps may occur. For example, these simulations deviated from the data at early time points (between 0 and 50 ms) for very positive potentials. This deviation suggested some additional delay, possibly due to additional closed states in the activation pathway. In addition, the holding potential used (−40 mV) in the ferret atrial I_{Kr} experiments of Liu *et al.* (1996) was very close to the threshold for activation of I_{Kr}. In fact, their model predicted that ~5% of the total current would be activated at this holding potential. This positive holding potential would decrease the degree of sigmoidicity (i.e. through Cole–Moore shifts (Cole & Moore, 1960)).

The activation data for this channel were suggestive of a voltage-insensitive step in the activation pathway. Such a

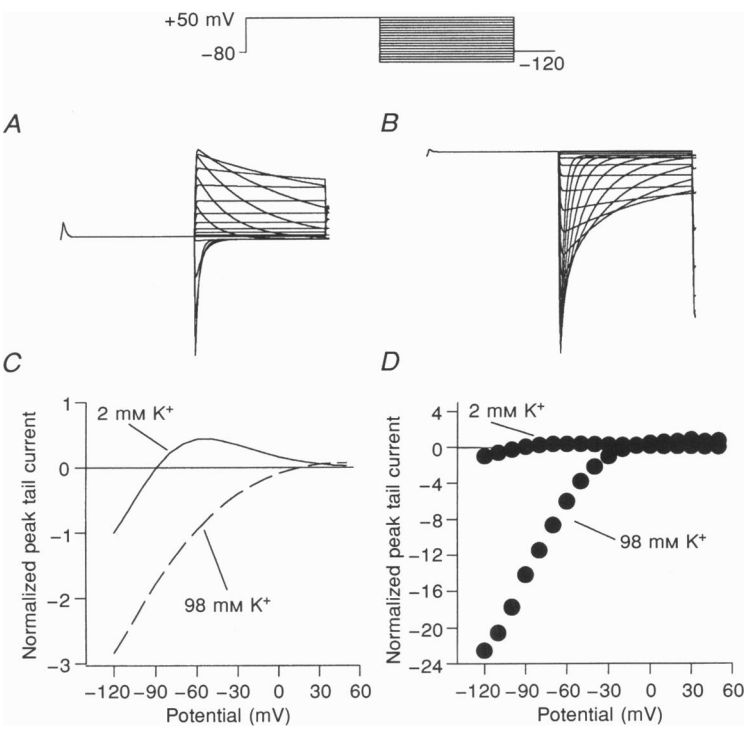

Figure 10. Degree of current activation due to changes in gating characteristics

A, simulation of peak tail currents assuming a linear instantaneous *I–V* relationship in 2 mM K_o^+. The holding potential was −80 mV. A depolarizing prepulse to +50 mV of 3000 ms duration was delivered to the oocytes before subsequently stepping to various potentials (−120 to +50 mV in 10 mV increments). *B*, simulations using the same protocol, assuming an identical linear conductance as *A* but with inactivation parameters and a reversal potential suitable for 98 mM K_o^+. *C*, simulated peak tail currents measured from panels *A* and *B*. The net model currents were normalized to the value of peak tail current for a P2 potential of −120 mV in 2 mM K_o^+. *D*, experimentally measured peak tail current in 2 and 98 mM K_o^+. The net experimentally measured currents were normalized to the value of peak tail current for a P2 potential of −120 mV in 2 mM K_o^+ for comparison with the simulation result. Note that the model without a change in 'open channel' conductance only accounts for a small fraction of the total increase in the experimentally observed current.

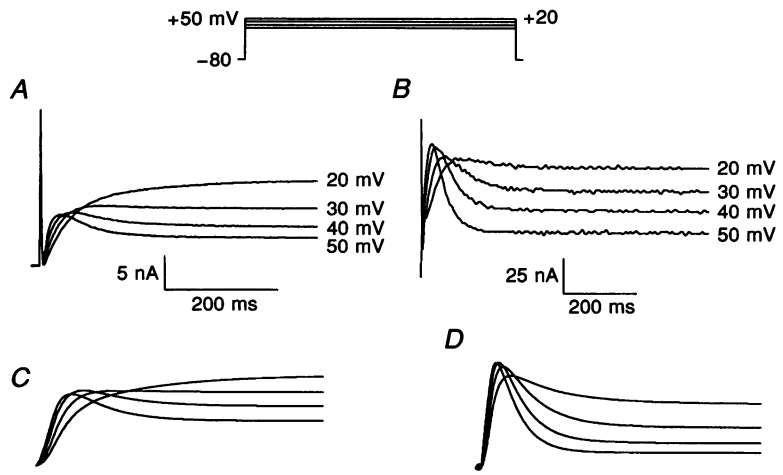

Figure 11. Data and simulations demonstrating a transient component of the I_{HERG} at positive potentials

A, early portion of I_{HERG} elicited in response to a step in potential from −80 to +20mV through +50 mV in 2 mM K_o^+. Data were leakage subtracted. *B*, data from same protocol but with 98 mM K_o^+. *C* and *D*, simulations of the data in *A* and *B*. These simulations included the measured instantaneous *I–V* relationship for the currents (Wang *et al.* 1996). Note the similarity in the time course of the transient between the simulated and measured data.

step preceding opening is unique to I_{Kr} and I_{HERG} among voltage-gated K^+ channels. Examination of the S4 sequence of the putative voltage-sensing region of HERG, provides little insight as to why activation should be so different in this channel as opposed to *Shaker* and the known mammalian homologues (Fig. 12). The positively charged residues are well conserved through most of the S4 region in all the different voltage-gated K^+ channels. However, near the end of the cytoplasmic side of S4 in HERG there is one charge reversal at position 540 and additional positive charges at positions 538 and 541. In addition, there is an aspartate residue at position 544. Potentially, the proximity of these charged residues may result in local neutralization of some of the voltage sensor through salt-bridge formation. Such interactions could potentially reduce the voltage sensitivity of some activation transitions involving the S4 voltage sensor of HERG. However, it is also possible that lipophilic or allosteric mechanisms are responsible for the voltage-insensitive step in HERG activation.

A recent study has demonstrated a strong dependence of the myocyte I_{Kr} deactivation process on external divalent cations (Ho, Earm, Lee, Brown & Noble, 1996). A simple open channel block model was proposed in which block by divalent ions mediated a fast voltage-dependent deactivation process. We performed preliminary studies in which $[Mg^{2+}]_o$ increased from 1 to 10 mM produced at best a modest increase in deactivation rate (from 293 ± 81 to 245 ± 60 ms, $n = 3$ at a deactivation potential of −100 mV) suggesting that the heterologously expressed channel may not have this same sensitivity to block by external divalent cations. This difference may reflect missing ancillary subunits or the presence of alternative splice variants of HERG in the native cells.

Inactivation

Previous studies have demonstrated that the rectification properties of I_{Kr} and I_{HERG} arise from a rapid inactivation process. This study includes the first complete quantitative characterization of the voltage dependence of macroscopic

Figure 12. Alignment of the sequence in the S4 and flanking regions of HERG relative to Kv1.4 and *Shaker*

The figure shows an alignment of the putative S4 voltage sensor (residues 518–544 for HERG, 355–381 for *Shaker* and 438–464 for Kv1.4). Note the disruption in the repeat of the last two positively charged residues near the C-terminal end of HERG and the presence of negatively charged residues near each end of S4. Sources of sequence information: HERG, Warmke & Ganetzky (1994); *Shaker*, Papazian, Schwarz, Tempel, Jan & Jan (1987) and Kv1.4, Comer *et al.* (1994).

HERG inactivation. Inactivation of HERG displayed interesting voltage sensitivity. Time-dependent inactivation of HERG has been previously shown to be strongly voltage dependent in the hyperpolarized range of potentials, with recovery from inactivation becoming faster with increasing hyperpolarization (Sanguinetti *et al.* 1995). Similarly, it has also been demonstrated that inactivation in the positive range of potentials is also strongly voltage dependent (Wang *et al.* 1996*a*,*b*). This study showed the classical 'bell-shaped' voltage dependence of the time constant of inactivation of HERG and that its behaviour could be well described by a simple voltage-dependent Hodgkin & Huxley (1952) type gating variable.

This 'bell-shaped' voltage dependence is distinct from both N-type and C-type inactivation mechanisms described for voltage-gated K^+ channels. In both *Shaker* and Kv1.4 channels C-type inactivation is a voltage-insensitive process at positive potentials (Hoshi *et al.* 1990; Rasmusson *et al.* 1995). Any apparent voltage dependence arises from direct coupling to activation. Such a coupling-type mechanism is unlikely to explain the voltage dependence noted here. Inactivation continues to be voltage dependent at potentials where activation is essentially complete. Two additional observations that suggest that the voltage dependence of inactivation does not arise from activation are: (1) the slopes of steady-state activation and inactivation relationships differ by more than a factor of two; and (2) the activation properties of HERG are insensitive to increased extracellular K^+ while the inactivation rate (Figs 1 and 2) and $V_{½}$ of inactivation are shifted positively by ~30 mV. The non-parallel properties of activation and inactivation are indicators that the voltage dependence of inactivation is independent of the voltage dependence of activation. Thus, inactivation of HERG has unique intrinsic voltage sensitivity similar to that observed for I_{Kr}.

Rapid inactivation of HERG is sensitive to 100 mM TEA (Smith *et al.* 1996), elevated extracellular potassium (Wang *et al.* 1996) and mutations near the exterior mouth of the channel (Smith *et al.* 1996; Schönherr & Heinemann, 1996) and is insensitive to N-terminal deletion (Spector *et al.* 1996; Schönherr & Heinemann, 1996). For these reasons, inactivation of HERG has been labelled C-type. However, our own and other studies reveal that HERG inactivation shows several properties that are biophysically distinct from 'classic' C-type inactivation. (1) The rate of recovery from C-type inactivation is generally thought to increase with increasing $[K^+]_o$ (Baukrowitz & Yellen, 1995; Rasmusson *et al.* 1995), in contrast to the rate of recovery of HERG inactivation which decreased with an increase of $[K^+]_o$. (2) The rate of development of C-type inactivation is voltage insensitive at potentials positive to the threshold for activation (Hoshi *et al.* 1990; Rasmusson *et al.* 1995); in contrast HERG inactivation is voltage sensitive at such potentials. (3) *Shaker* and Kv1.4 mutant channels that have a fast rate of development of C-type inactivation usually have a slow rate of recovery (Hoshi *et al.* 1990; Lopez-Barneo, Hoshi, Heinemann & Aldrich, 1993; Rasmusson *et al.* 1995); HERG has both a rapid development of C-type inactivation and a rapid recovery from inactivation. Thus, the inactivation mechanism of the HERG channel shows several unique properties that contrast with the properties described for C-type inactivation in other channels. This raises the possibility that the term C-type inactivation may include more than one distinct mechanism (e.g. P-type inactivation; DeBiasi, Hartmann, Drewe, Taglialatela, Brown & Kirsch, 1993).

Physiological implications

The physiological importance of *HERG* to the repolarization of cardiac muscle is well established because of the link between mutations in this gene and an inherited form of long QT syndrome (Curran *et al.* 1995). The native current attributed to this gene product, I_{Kr}, has been difficult to study in many native cell types, including human cardiac myocytes, because it is small compared with other overlapping K^+ currents (e.g. I_{K1}, I_{Ks} and I_{Kur}) (Wang *et al.* 1993; Wang, Fermini & Nattel 1994; Muraki *et al.* 1995; Liu *et al.* 1996). This has made quantitative analysis of many of its kinetic properties difficult at best. Unfortunately, the time and voltage dependence of currents are the determining factor in their physiological role in the regulation of action potential repolarization. Our study validates two novel types of time- and voltage-dependent behaviour of I_{Kr} as measured through E-4031-sensitive currents. First, a slow sigmoid time course of activation of I_{HERG} currents at positive potentials was established that matched the previously observed kinetics for the native channel (Liu *et al.* 1996). The sigmoidicity measured for HERG required more states to reproduce than was required for native ferret I_{Kr}, but this quantitative difference most likely reflects the better isolation of I_{HERG} from overlapping currents in the cloned channel. More negative holding potentials (−80 to −120 mV for oocytes *vs.* −40 mV for myocytes) would tend to maximize Cole–Moore shifts in the sigmoidicity of activation. Second, a transient outward peak of current was observed during sudden depolarization to positive potentials similar to that observed in ferret atrial myocytes (Liu *et al.* 1996). The observation of these parallel results in the cloned channel analogue of I_{Kr} strengthens the confidence that the drug-sensitive current behaviour in native myocytes reflects the behaviour of a single well-isolated channel type.

Anumonwo, J. M. B., Freeman, L. C., Kwok, W. M. & Kass, R. S. (1992). Delayed rectification in single cells isolated from guinea pig sinoatrial node. *American Journal of Physiology* **262**, H921–925.

Balser, J. R., Bennett, P. B. & Roden, D. M. (1990). Time-dependent outward current in guinea pig ventricular myocytes. *Journal of General Physiology* **96**, 835–863.

Baukrowitz, T. & Yellen, G. (1995). Modulation of K^+ current by frequency and external $[K^+]$: a tale of two inactivation mechanisms. *Neuron* **15**, 951–960.

CAMPBELL, D. L., RASMUSSON, R. L., QU, Y. & STRAUSS, H. C. (1993). The calcium-independent transient outward potassium current in isolated ferret right ventricular myocytes. *Journal of General Physiology* **101**, 571–601.

CAMPBELL, D. L., RASMUSSON, R. L. & STRAUSS, H. C. (1992). Ionic current mechanisms generating vertebrate primary pacemaker activity at the single cell level: an integrative view. *Annual Review of Physiology* **54**, 279–302.

CARMELIET, E. (1992). Voltage- and time-dependent block of the delayed K^+ current in cardiac myocytes by dofetilide. *Journal of Pharmacology and Experimental Therapeutics* **262**, 809–817.

CARMELIET, E. (1993). Use-dependent block and use-dependent unblock of delayed rectifier K^+ current by amokalant in rabbit ventricular myocytes. *Circulation Research* **73**, 857–868.

CASTELLINO, R. C., MORALES, M. J., STRAUSS, H. C. & RASMUSSON, R. L. (1995). Time- and voltage-dependent modulation of a Kv1.4 channel by a β-subunit (Kvβ3) cloned from ferret ventricle. *American Journal of Physiology* **269**, H385–391.

CLAY, J. R., OGBAGHEBRIEL, A., PAQUETTE, T., SASYNIUK, B. I. & SHRIER, A. (1995). A quantitative description of the E-4031 sensitive repolarization current in rabbit ventricular myocytes. *Biophysical Journal* **69**, 1830–1837.

COLE, K. S. & MOORE, J. W. (1960). Potassium ion current in the squid giant axon. Dynamic characteristics. *Biophysical Journal* **1**, 1–14.

COMER, M. B., CAMPBELL, D. L., RASMUSSON, R. L., LAMSON, D. R., MORALES, M. J., ZHANG, Y. & STRAUSS, H. C. (1994). Cloning and expression of an I_{to}-like potassium channel from ferret ventricle. *American Journal of Physiology* **267**, H1383–1395.

CURRAN, M. E., SPLAWSKI, I., TIMOTHY, K. W., VINCENT, G. M., GREEN, E. D., & KEATING M. T. (1995). A molecular basis for cardiac arrhythmia: *HERG* mutations cause long QT syndrome. *Cell* **80**, 795–803.

DEBIASI, M., HARTMANN, H. A., DREWE, J. A., TAGLIALATELA, M., BROWN, A. M. & KIRSCH, G. E. (1993). Inactivation determined by a single site in K^+ pores. *Pflügers Archiv* **422**, 354–363.

DIFRANCESCO, D. (1985). The cardiac hyperpolarizing-activated current, i_f. Origins and developments. *Progress in Biophysics and Molecular Biology* **46**, 163–183.

HO, W. K., EARM, Y. E., LEE, S. K., BROWN, H. F. & NOBLE, D. (1996). Voltage- and time-dependent block of delayed rectifier K^+ current in rabbit sino-atrial node cells by external Ca^{2+} and Mg^{2+}. *Journal of Physiology* **494**, 727–742.

HODGKIN, A. L. & HUXLEY, A. F. (1952). A quantitative description of membrane current and its application to conduction and excitation in nerve. *Journal of Physiology* **117**, 500–544.

HOSHI, T., ZAGOTTA, W. N. & ALDRICH, R. W. (1990). Biophysical and molecular mechanisms of *Shaker* potassium channel inactivation. *Science* **250**, 533–538.

HOSHI, T., ZAGOTTA, W. N. & ALDRICH, R. W. (1994). *Shaker* potassium channel gating I: transitions near the open state. *Journal of General Physiology* **103**, 249–278.

JURKIEWICZ, N. K. & SANGUINETTI, M. C. (1993). Rate dependent prolongation of cardiac action potentials by a methanesulfamilide agent. Specific block of rapidly activating delayed rectifier K^+ current by dofetilide. *Circulation Research* **72**, 75–83.

KIEHN, J., LACERDA, A., WIBLE, B., SANGUINETTI, M., KEATING, M. & BROWN, A. M. (1996). Single channel properties of HERG, the channel encoding I_{Kr}. *Biophysical Journal* **70**, A361.

LIU, S., RASMUSSON, R. L., CAMPBELL, D. L., WANG, S. & STRAUSS, H. C. (1996). Activation and inactivation kinetics of an E-4031 sensitive current (I_{Kr}) from single ferret atrial myocytes. *Biophysical* JOURNAL **70**, 2704–2715.

LÓPEZ-BARNEO, L., HOSHI, T., HEINEMANN, S. H. & ALDRICH, R. W. (1993). Effects of external cations and mutations in the pore region on C-type inactivation of *Shaker* potassium channels. *Receptors and Channels* **1**, 61–71.

MCALLISTER, R. E., NOBLE, D. & TSIEN, R. W. (1975). Reconstruction of the electrical activity of cardiac Purkinje fibers. *Journal of Physiology* **251**, 1–59.

MURAKI, K., IMAIZUMI, Y., WATANABE, M., HABUCHI, Y. & GILES, W. R. (1995). Delayed rectifier K^+ current in rabbit atrial muscle. *American Journal of Physiology* **269**, H524–532.

NOBLE, D. (1984). The surprising heart: A review of recent progress in cardiac electrophysiology. *Journal of Physiology* **353**, 1–50.

PAPAZIAN, D. M., SCHWARZ, T. L., TEMPEL, B. L., JAN, Y. N. & JAN, L. Y. (1987). Cloning of genomic and complementary DNA from *Shaker*, a putative potassium channel gene from *Drosophila*. *Science* **237**, 749–753.

RASMUSSON, R. L., MORALES, M. J., CASTELLINO, R. C., ZHANG, Y., CAMPBELL, D. L. & STRAUSS, H. C. (1995). C-type inactivation controls recovery in a fast inactivating cardiac K^+ channel (Kv1.4). *Journal of Physiology* **489**, 709–721.

SANGUINETTI, M. C., JIANG, C., CURRAN, M. E. & KEATING, M. T. (1995). A mechanistic link between an inherited and an acquired cardiac arrhythmia: HERG encodes the I_{Kr} potassium channel. *Cell* **81**, 299–307.

SANGUINETTI, M. C. & JURKIEWICZ, N. K. (1990). Two components of cardiac delayed rectifier K^+ current. Differential sensitivity to block by class III antiarrhythmic agents. *Journal of General Physiology* **96**, 195–215.

SCHÖNHERR, R. & HEINEMANN, S. H. (1996). Molecular determinants for activation and inactivation of HERG, a human inward rectifier potassium channel. *Journal of Physiology* **493**, 635–642.

SHIBASAKI, T. (1987). Conductance and kinetics of delayed rectifier potassium channels in nodal cells of the rabbit heart. *Journal of Physiology* **387**, 227–250.

SHIBATA, E. F. & GILES, W. R. (1985). Ionic currents which generate the spontaneous diastolic depolarizations in individual cardiac pacemaker cells. *Proceedings of the National Academy of Science of the USA* **82**, 7796–7800.

SMITH, P. L., BAUKROWITZ, T. & YELLEN, G. (1996). The inward rectification mechanism of the HERG cardiac potassium channel. *Nature* **379**, 833–836.

SPECTOR, P. M., CURRAN, M. E., ZOU, A. R. & SANGUINETTI, M. C. (1996). Fast inactivation causes rectification of the I_{Kr} channel. *Journal of General Physiology* **107**, 611–619.

TAGLIALATELA, M., TORO, L. & STEFANI, E. (1992). Novel voltage clamp to record small, fast currents from ion channels expressed in *Xenopus* oocytes. *Biophysical Journal* **61**, 78–82.

TRUDEAU, M. C., WARMKE, J. W., GANETZKY, B. & ROBERTSON, G. A. (1995*a*). HERG, a human inward rectifier in the voltage-gated potassium channel family. *Science* **269**, 92–95.

TRUDEAU, M. C., WARMKE, J. W., GANETZKY, B. & ROBERTSON, G. A. (1995*b*). HERG sequence correction. *Science* **272**, 1087.

VERHEIJCK, E. E., VAN GINNEKEN, A. C. G., BOURIER, J. & BOUMAN, L. N. (1995). Effects of delayed rectifier current blockade by E-4031 on impulse generation in single sinoatrial nodal myocytes of the rabbit. *Circulation Research* **76**, 607–615.

WANG, J., TRUDEAU, M. C. & ROBERTSON, G. A. (1996*a*). Inactivation and external potassium sensitivity in HERG potassium channels. *Biophysical Journal* **70**, A97.

Wang, S., Morales, M. J., Liu, S., Strauss, H. C. & Rasmusson, R. L. (1996*b*). Time-, voltage- and ionic-concentration dependence of rectification of h-*erg* expressed in *Xenopus* oocytes. *FEBS Letters* **389**, 167–173.

Wang, Z., Fermini, B. & Nattel, S. (1993). Delayed rectifier outward current and repolarization in human atrial myocytes. *Circulation Research* **73**, 276–285.

Wang, Z., Fermini, B. & Nattel, S. (1994). Rapid and slow components of delayed rectifier current in human atrial myocytes. *Cardiovascular Research* **28**, 1540–1546.

Warmke, J. W. & Ganetzky, B. (1994). A family of potassium channel genes related to *eag* in *Drosophila* and mammals. *Proceedings of the National Academy of Sciences of the USA* **91**, 3438–3442.

Yang, T., Snyders, D. J. & Roden, D. M. (1996). Extracellular potassium modulates the gating, but not the rectification, of the rapidly-activating cardiac delayed rectifier I_{Kr}. *Biophysical Journal* **70**, A276.

Acknowledgements

We gratefully acknowledge the technical support of Ann Crews and Douglas Opel. This work was supported in part by a NIH grant no. HL-19216 and a Biomedical Engineering Research Grant from the Whitaker Foundation.

Author's email address

R. L. Rasmusson: raz@acpub.duke.edu

Received 16 December 1996; accepted 9 April 1997.